



## City Research Online

### City, University of London Institutional Repository

---

**Citation:** Rokni, H., Gupta, A., Moore, J., McHugh, M. A., Bamgbade, B. & Gavaises, M. (2019). Purely predictive method for density, compressibility, and expansivity for hydrocarbon mixtures and diesel and jet fuels up to high temperatures and pressures. *Fuel*, 236, pp. 1377-1390. doi: 10.1016/j.fuel.2018.09.041

This is the accepted version of the paper.

This version of the publication may differ from the final published version.

---

**Permanent repository link:** <https://openaccess.city.ac.uk/id/eprint/21722/>

**Link to published version:** <https://doi.org/10.1016/j.fuel.2018.09.041>

**Copyright:** City Research Online aims to make research outputs of City, University of London available to a wider audience. Copyright and Moral Rights remain with the author(s) and/or copyright holders. URLs from City Research Online may be freely distributed and linked to.

**Reuse:** Copies of full items can be used for personal research or study, educational, or not-for-profit purposes without prior permission or charge. Provided that the authors, title and full bibliographic details are credited, a hyperlink and/or URL is given for the original metadata page and the content is not changed in any way.

---

City Research Online:

<http://openaccess.city.ac.uk/>

[publications@city.ac.uk](mailto:publications@city.ac.uk)

---

Article

**Corresponding Author:**

Houman Rokni, Afton Chemical Ltd., Bracknell, Berkshire, RG12 2UW, UK & Department of Mechanical Engineering and Aeronautics, City University of London, Northampton Square, EC1V 0HB London, UK

Email: [houman.rokni@aftonchemical.com](mailto:houman.rokni@aftonchemical.com)

# Purely predictive method for density, compressibility, and expansivity for hydrocarbon mixtures and diesel and jet fuels up to high temperatures and pressures

Houman B. Rokni<sup>1,2</sup>, Ashutosh Gupta<sup>3</sup>, Joshua D. Moore<sup>3</sup>, Mark A. McHugh<sup>4</sup>, Babatunde A. Bamgbade<sup>4</sup>, and Manolis Gavaises<sup>2</sup>

<sup>1</sup>Afton Chemical Ltd., Bracknell, Berkshire, RG12 2UW, UK

<sup>2</sup>Department of Mechanical Engineering and Aeronautics, City, University of London, Northampton Square, EC1V 0HB London, UK

<sup>3</sup>Afton Chemical Corp., Richmond, Virginia 23219, USA

<sup>4</sup>Department of Chemical and Life Science Engineering, Virginia Commonwealth University, Richmond, Virginia 23284, USA

## Abstract

This study presents a pseudo-component method using the Perturbed-Chain Statistical Associating Fluid Theory to predict density, isothermal compressibility, and the volumetric thermal expansion coefficient (expansivity) of hydrocarbon mixtures and diesel and jet fuels. The model is not fit to experimental density data but is predictive to high temperatures and pressures using only two calculated or measured mixture properties as inputs: the number averaged molecular weight and hydrogen to carbon ratio. Mixtures are treated as a single pseudo-component; therefore binary interaction parameters are not needed. Density is predicted up to 470 K and 3,500 bar for hydrocarbon mixtures and fuels with 1% average mean absolute percent deviation (MAPD). Isothermal compressibility is predicted with 4% average MAPD for hydrocarbon mixtures and 9% for fuels. The volumetric thermal expansion coefficient is predicted with 7% average MAPD for hydrocarbon mixtures and 13% for fuels.

Keywords: PC-SAFT, Diesel fuel, Density, Derivative properties, Pseudo-component, High pressures

## 1 Introduction

Diesel and jet engines remain the predominant combustion technologies for the heavy duty, automotive, and aviation sectors, due to their performance and fuel economy [1-4].

The need for improved fuel economy and increasingly stringent emission regulations have motivated diesel and jet engine manufacturers to optimize fuel injection equipment (FIE) design. Sophisticated and complex FIE systems not only have to perform at extreme operating conditions but also need to be robust. They need to ensure performance for diesel and jet fuels that vary in composition in different markets.

Experimental development, testing, and validation of these technologies is a significant time and resource-intensive process.

To accelerate this process and reduce costs, computational fluid dynamics (CFD) simulations are routinely used by manufacturers to evaluate, understand, and optimize FIE design and operation. Many numerical methods and approaches have been developed to simulate the performance of fuel injectors and provide insight into the physical processes taking place inside these systems [5-19]. Accurate simulation of the flow field within the FIE and phenomena observed further downstream (e.g., jet breakup and spray formation) is required to ensure their reliable predictive capability. In an approach to meet stringent fuel economy and emission targets, FIE manufacturers are developing new diesel injector designs that operate at pressures up to 4,500 bar [20] to achieve improved flow and spray performance.

Accurate simulations of the flow field are dependent on accurate representations of thermophysical properties of the fuel (e.g., density, isothermal compressibility, volumetric thermal expansion coefficient). A recent CFD study [21] predicted up to 7%

variation in mass flow rate through diesel injectors when accounting for the temperature and pressure dependence of thermophysical properties in the model. Local temperatures were shown to increase by as much as 180 °C when fuel was discharged through diesel injectors, due to significant friction induced heating near the injector walls, which overcame cooling effects that occur due to depressurization. CFD has been used to demonstrate temperature and pressure effects on nozzle flow and cavitation [22], fuel vaporization [23], and spray distribution [24]. Thermophysical property models of fuels are needed to accurately predict their high temperature and high pressure (HTHP) behavior.

Experimental measurement of fuel properties at HTHP are expensive and time consuming, and data are often not available. These limitations can be overcome using an equation of state (EoS) to calculate mixture properties beyond the range of experimental observations. Among the general classes of EoS used in modeling properties of hydrocarbon mixtures are cubic EoS (e.g., Peng Robinson (PR) and Soave–Redlich–Kwong (SRK) [21-23]). Another class of EoS are those based on the Statistical Associating Fluid Theory (SAFT) [24-27], generally acknowledged as superior in predictive ability [28-32]. Many modifications to the original SAFT EoS have been proposed, with perhaps the most widely used in industry being the Perturbed-Chain SAFT (PC-SAFT) EoS of Gross and Sadowski [33].

The computational time for a CFD simulation increases significantly, often non-linearly, with the number of components in a mixture. Often, a small number of components are chosen as a surrogate mixture to closely match the thermophysical properties of the fuel [34-41]. Despite the relative computational simplicity surrogates may offer, selection of

the individual components and their concentrations is difficult and involves a significant amount of manual effort. Furthermore, since the surrogate mixture is optimized for a specific fuel, this mixture cannot be expected to predict the properties of another fuel with a different composition.

Another approach is to represent a complex mixture (e.g., fuels, crude oils) through one or more pseudo-components [42-47]. Ting [46] modeled the phase behavior of crude oil using three pseudo-components representing saturates (e.g., alkanes and naphthenes), aromatics, and asphaltenes. Ting correlated the PC-SAFT parameters to molecular weight (MW) and calculated parameters for the three pseudo-components using a weighted averaging term, defined as aromaticity. Ting [46] fit aromaticity to the bubble-point pressure and defined it to vary from 0 for poly-nuclear aromatics (PNAs) to 1 for benzene derivatives (BDs). Gonzalez [44] modified the PC-SAFT correlations reported by Ting [46] and redefined the range of aromaticity from 0 for BDs to 1 for PNAs. Punnapala and Vargas [45] fit aromaticity to the saturated liquid density and bubble-point pressure and redefined the range of it from 0 for normal alkanes (n-alkanes) to 1 for PNAs. The redefined range of Punnapala and Vargas provided better phase behavior predictions for crude oils.

Abutaqiya et al. [42] studied several crude oils and predicted density and phase behavior using a single pseudo-component. They used the PC-SAFT correlations proposed by Gonzalez and fit aromaticity to experimental saturated liquid density and bubble-point pressure. Burgess et al. [47] fit correlations for the PC-SAFT parameters to high temperature and high pressure (HTHP) experimental data [48] and predicted density for two crude oils. To make the approach predictive, they calculated aromaticity from the

hydrogen to carbon (HN/CN) ratio of the fuel obtained from elemental analysis using a definition proposed by Huang and Radosz [27].

Previous techniques for predicting density and derivative properties for complex mixtures have been limited by the need for experimental measurements to fit the EoS parameters or requiring complex compositional characterization to define multiple pseudo-components. This study describes the development of a single, pseudo-component technique using the PC-SAFT EoS to predict density, isothermal compressibility, and the volumetric thermal expansion coefficient for hydrocarbon mixtures without the need for fitted binary interaction parameters. Two mixture properties are required for the predictions: the number averaged MW and the HN/CN ratio, both of which are either calculated when working with well-defined, simple mixtures or are measured when working with multicomponent fuel mixtures. The present technique utilizes the HTHP group contribution (GC) parameters developed by Burgess et al. [49] to correlate the PC-SAFT parameters with respect to MW. The PC-SAFT parameters of the pseudo-component are then determined using the mixture HN/CN ratio in a modified averaging equation previously used by other researchers [50-54]. Fluid property predictions are compared to experimental data for six hydrocarbon mixtures with varying composition to demonstrate the technique. Further predictions are then presented for four diesel fuels and two jet fuels over a wide range of temperatures and pressures to more fully explore the capabilities of the pseudo-component technique with a focus on HTHP fluid properties.

## 2 Technique Development

### 2.1 Perturbed-Chain Statistical Associating Fluid Theory (PC-SAFT)

The PC-SAFT EoS, developed by Gross and Sadowski [33], is molecularly based and accounts for the effects of molecular size, molecular shape, dispersion forces, and association of molecules. Details of the EoS can be found elsewhere [33]. In the present study, contribution of the association term is neglected since the compounds in the fuels and hydrocarbon mixtures do not exhibit association, such as hydrogen bonding. The residual, reduced Helmholtz free energy ( $\tilde{a}^{res}$ ) of the pseudo-component is expressed as:

$$\tilde{a}^{res} = \tilde{a}^{hc} + \tilde{a}^{disp} \quad (1)$$

where  $\tilde{a}^{hc}$  and  $\tilde{a}^{disp}$  are the contributions of the hard chain and dispersion reduced Helmholtz free energies, respectively.

Pure-component PC-SAFT parameters (i.e.,  $m$ , the number of segments per chain;  $\sigma$ , the segment diameter; and  $\varepsilon/k$ , the depth of the potential well) are generally fit to vapor pressure and saturated liquid density data [33]. They also can be determined from group contribution (GC) methods [55-57]. The GC parameters from most methods are not fit to high pressure data and lead to property predictions which deviate at high pressures [56-61]. Since Burgess et al. [49] fit their GC parameters to HTHP density data, and their parameters are used in this study.

### 2.1 Pseudo-component Technique

The GC parameters published by Burgess et al. [49] are used to calculate the PC-SAFT parameters of the 140 compounds reportedly found in two different diesel fuels [35].

Figure 1 shows the variation of  $m$  with respect to MW for this range of compounds,

although only selected compounds from the different chemical families in the diesel fuel are shown to avoid a cluttered graph. For a given MW,  $m$  appears to be a function of molecular structure with n-alkanes and PNAs bounding the distribution. Similar trends are observed for the other PC-SAFT parameters,  $m\sigma$  and  $\epsilon k$ . These observations are consistent with those reported by Huang and Radosz [27] and Gonzalez [44] who developed parameter correlations based on pure component parameters fit to vapor pressure and saturated liquid density.

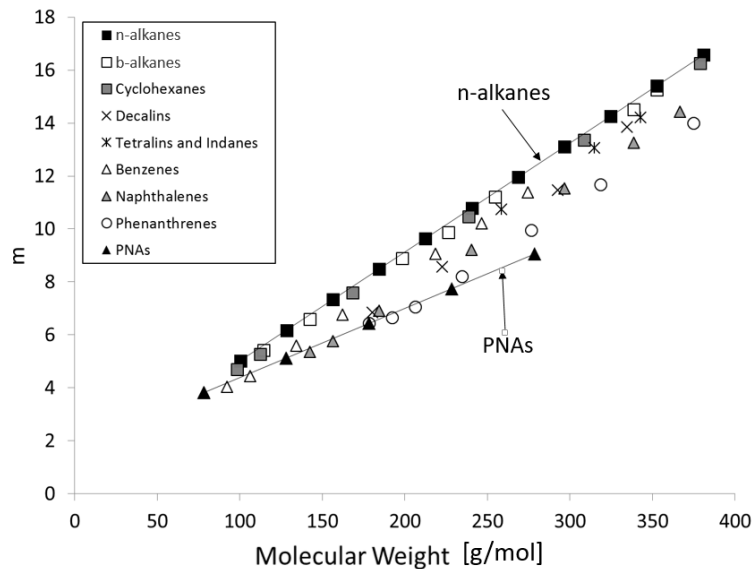


Figure 1: PC-SAFT  $m$  segment parameter of selected components calculated using GC parameters of Burgess et al. [49].

Figure 2 shows the PC-SAFT parameters for the two bounds, n-alkanes and PNAs, as functions of MW. Selected n-alkanes and PNAs are shown to avoid a cluttered graph. Table 1 lists correlations for  $m$ ,  $m\sigma$  and  $\epsilon k$ , as a function of MW. The correlations for the PC-SAFT parameters fit in this study are comparable to those by Burgess et al. [47] but extend the range of MWs to approximately 500 g/mol for n-alkanes and approximately

300 g/mol for PNAs. This higher MW range covers the broad range of compounds typically found in diesel fuels and, therefore, avoids the need for extrapolation.

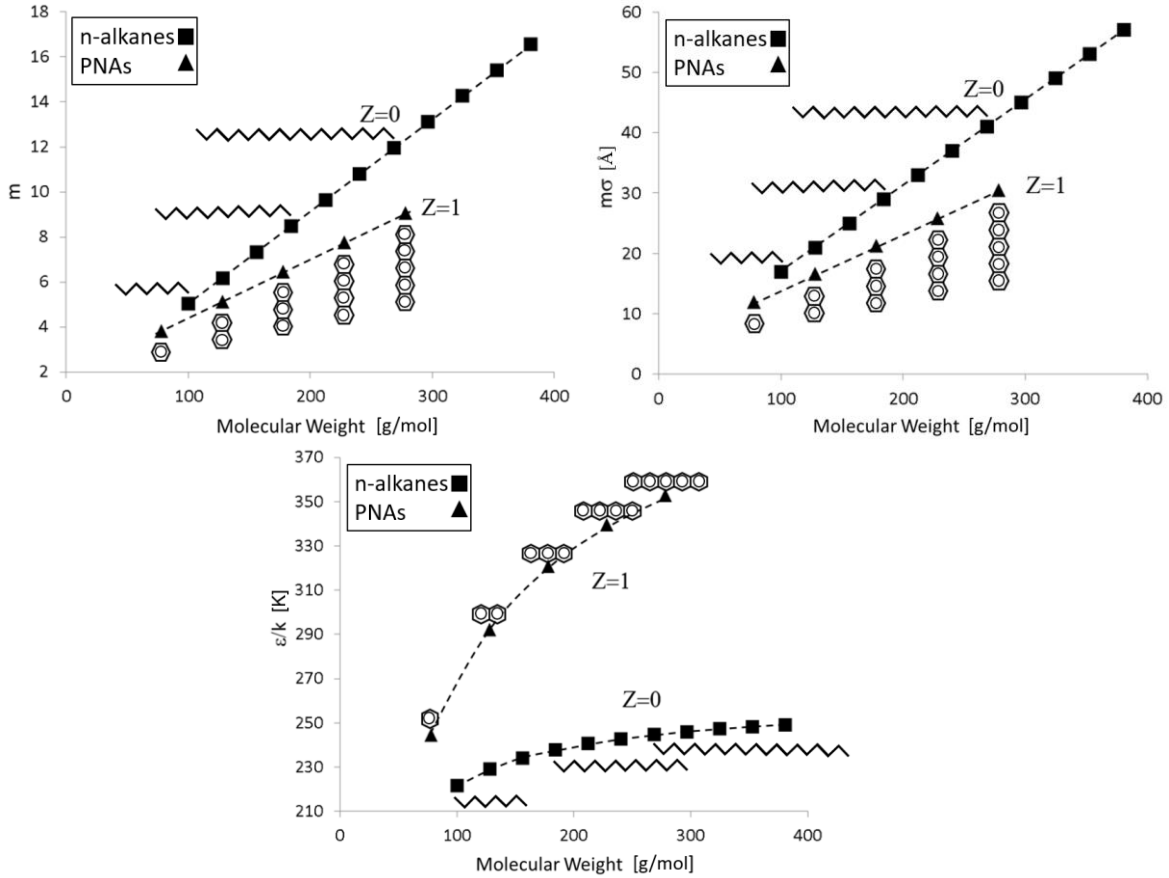


Figure 2: PC-SAFT parameters calculated using GC parameters of Burgess et al. [49] as a function of MW for n-alkanes and PNAs. The structures of representative molecules are shown on the figures. The degree of unsaturation of a mixture is represented through a parameter  $Z$  and is described in the text.  $Z$  varies from 0 for n-alkanes to 1 for PNAs.

	n-alkanes	PNAs
$m$	$0.0412MW + 0.8954$	$0.0262MW + 1.7750$
$m\sigma$ [Å]	$0.1430MW + 2.5847$	$0.0922MW + 4.7925$
$\varepsilon/k$ [K]	$\exp^{(5.5599 - 16.1830/MW)}$	$\exp^{(6.0022 - 39.8810/MW)}$

Table 1: PC-SAFT parameter correlations as a function of MW (g/mol) for n-alkanes and PNAs used in this study.

The pseudo-component PC-SAFT parameters need to account for the MWs and the degree of unsaturation of the compounds in the mixture. The MWs of all the compounds in the mixture are averaged to obtain the mixture number averaged MW. Here the degree of unsaturation (DoU) of compounds in a mixture is normalized and calculated in Eq. 2 as the parameter  $Z$ .  $Z$  varies from 0 for n-alkanes to 1 for PNAs as shown in Figure 2. Since the DoU of n-alkanes is zero,  $Z$  reduces to the degree of unsaturation of the mixture divided by the degree of unsaturation of a PNA with a MW equal to the mixture number averaged MW. The correlation of  $\text{DoU}_{PNA}$  as a function of MW, shown in the supplementary information (SI), is used to calculate a value for  $\text{DoU}_{PNA}$  needed in Eq. 2.

$$Z = \frac{\text{DoU}_{mixture} - \text{DoU}_{n-alkane}}{\text{DoU}_{PNA} - \text{DoU}_{n-alkane}} = \frac{\text{DoU}_{mixture}}{\text{DoU}_{PNA}} \quad (2)$$

$\text{DoU}_{mixture}$  is calculated by Eq. 3 from the average carbon number (CN) and average hydrogen number (HN) of the mixture. The hydrogen to carbon ratio, HN/CN can either be calculated if all of the mixture components are known or can be obtained from elemental analysis when dealing with a complex fuel mixture.

$$\text{DoU} = \frac{1}{2}(2 \times \text{CN} + 2 - \text{HN}) \quad (3)$$

Similar to the aromaticity parameter used by Punnapala and Vargas [45], the  $Z$  parameter is used to average the contributions of the two bounds (i.e., n-alkanes and PNAs) for each pseudo-component PC-SAFT parameter, Eq. 4-6.

$$m_{mixture} = (1 - Z)m_{n-alkane} + Zm_{PNA} \quad (4)$$

$$(m\sigma)_{mixture} = (1 - Z)(m\sigma)_{n-alkane} + Z(m\sigma)_{PNA} \quad (5)$$

$$\left(\frac{\varepsilon}{k}\right)_{mixture} = (1 - Z)\left(\frac{\varepsilon}{k}\right)_{n-alkane} + Z\left(\frac{\varepsilon}{k}\right)_{PNA} \quad (6)$$

The hydrocarbon mixtures and diesel and jet fuels in this study do not contain compounds with DoUs greater than 10 (i.e., phenanthrene). However, DoUs greater than 10 would be calculated for PNAs using the  $DoU_{PNA}$  correlation as a function of MW if the mixture number average MW is greater than that for phenanthrene (i.e. 178 g/mol). Thus, direct application of Eq. 2 could underpredict the Z parameter. Instead, an upper bound of 10 is assigned for the DoU of PNAs when the mixture number averaged MW is greater than 178 g/mol, and the Z parameter is redefined as shown in Eq. 7.

$$Z = \begin{cases} \frac{DoU_{mixture}}{DoU_{PNA}}, MW_{mixture} < 178 \text{ g/mol} \\ \frac{DoU_{mixture}}{10}, MW_{mixture} \geq 178 \text{ g/mol} \end{cases} \quad (7)$$

The PC-SAFT parameters of the pseudo-component can be calculated using a combination of either the original expression for the Z parameter (Eq. 2) or the alternative expression (Eq. 7). Both approaches are used in the following property predictions for well-characterized hydrocarbon mixtures, four diesel fuels, and two jet fuels. PC-SAFT fluid property calculations are performed using the VLXE/Blend software [62]. For clarity only the isotherms at the lowest and highest temperatures are shown. However, the reported statistical measures include data at all temperatures available for the literature experimental data. Deviation plots are included in the SI. Statistical measures reported include percent deviation, maximum deviation (Max D), standard deviation (SD), MAPD, and bias. These are defined by Eq. 8-12.

$$Deviation (\%) = 100 \times \frac{(y_{Predict} - y_{Exp})}{y_{Exp}} \quad (8)$$

$$Max D (\%) = Max \left( 100 \times \frac{|y_{Predict} - y_{Exp}|}{y_{Exp}} \right) \quad (9)$$

$$SD (\%) = \sqrt{\frac{\sum (y - \bar{y})^2}{N - 1}} \quad (10)$$

$$MAPD (\%) = \frac{1}{N} \sum 100 \times \frac{|y_{Predict} - y_{Exp}|}{y_{Exp}} \quad (11)$$

$$Bias (\%) = \frac{1}{N} \sum 100 \times \frac{(y_{Predict} - y_{Exp})}{y_{Exp}} \quad (12)$$

In Eq. 8-12,  $y_{Exp}$ ,  $y_{Predict}$ ,  $N$ , and  $\bar{y}$  denote the experimental data point, the prediction, number of data points, and the mean, respectively.

### 3 Hydrocarbon Mixtures

Table 2 lists the composition of the six hydrocarbon mixtures used to evaluate the pseudo-component technique presented here. Baylaucq et al. [63] reported densities for binary mixtures of methyl-cyclohexane (MCH) and n-heptane for five different compositions for 3 isotherms at 303, 323, and 343 K and pressures up to 1,000 bar. Ijaz [64] reported densities of a ternary and two quaternary mixtures for 7 isotherms between 298 and 448 K and pressures up to 1,350 bar. Boned et al.[65] measured densities for a ternary and a quinary mixture for 7 isotherms between 293 to 353 K and pressures up to 1,000 bar. Table 3 presents the calculated MW, HN/CN ratio, Z parameter, and the PC-SAFT parameters of the pseudo-components for the six different hydrocarbon mixtures using both combinations of approaches to calculate Z.

Compounds	M1	M2	M3	M4	M5	M6
n-heptane	0.5 to 1.0	-	-	-	-	-
methyl-cyclohexane	balance	-	-	-	-	-
n-tridecane	-	-	-	-	0.394	0.200
2,2,4,4,6,8,8-hepta-methyl-nonane	-	-	-	-	-	0.162
heptyl-cyclohexane	-	-	-	-	0.348	0.353
heptyl-benzene	-	-	-	-	0.258	0.156
1-methyl-naphthalene	-	-	-	-	-	0.129
n-octane	-	0.460	0.349	0.347	-	-
n-dodecane	-	0.309	0.235	0.235	-	-
n-hexadecane	-	0.232	0.176	0.175	-	-
bi-cyclohexyl	-	-	0.241	-	-	-
di-isopropyl-benzene	-	-	-	0.244	-	-

Table 2. Molar composition of hydrocarbon mixtures studied in this work.

Sample	PC-SAFT parameters						
	MW	HN/CN	$Z$		$m$	$\sigma$ (Å)	$\epsilon/k$ (K)
M1 (1.000 mole fraction n-C <sub>7</sub> )	100.2	2.29	Original	0	5.0237	3.3667	221.08
M1 (0.875 mole fraction n-C <sub>7</sub> )	99.9	2.25	Original	0.0236	4.9985	3.3630	222.16
M1 (0.750 mole fraction n-C <sub>7</sub> )	99.7	2.21	Original	0.0472	4.9734	3.3592	223.24
M1 (0.625 mole fraction n-C <sub>7</sub> )	99.4	2.18	Original	0.0711	4.9484	3.3553	224.31
M1 (0.500 mole fraction n-C <sub>7</sub> )	99.2	2.14	Original	0.0950	4.9235	3.3514	225.39
M2	157.6	2.20	Original	0	7.3872	3.4000	234.47
M3	159.7	2.11	Original	0.0439	7.4069	3.3967	238.27
M4	158.7	2.03	Original	0.0971	7.2882	3.3912	242.33
M5	181.6	1.94	Original	0.1363	8.1219	3.3972	249.42
			Alternative	0.1390	8.1169	3.3969	249.65
M6	183.6	1.84	Original	0.2027	8.0768	3.3923	255.49
			Alternative	0.2092	8.0644	3.3917	256.06

Table 3. Mixture properties and PC-SAFT parameters of the pseudo-components for hydrocarbon mixtures predicted in this study. When the number averaged MW of the mixture is less than the MW of phenanthrene, Eq. 7 reduces to Eq. 2, and the original and alternative  $Z$  parameters are the same.

Figure 3 shows density predictions for the hydrocarbon mixtures reported by Baylaucq et al. [63], Ijaz [64], and Boned et al. [65] at the lowest and highest temperatures reported and pressures up to 1,350 bar. For brevity, only the composition containing 0.750 mole fraction n-heptane and 0.250 mole fraction MCH are reported in Figure 3. The predictions show quantitative agreement with experiment across all temperatures and pressures for all six mixtures. Only predictions using the original Z equation are shown for the M1-M4 mixtures, since their number averaged MWs are less than the MW of phenanthrene.

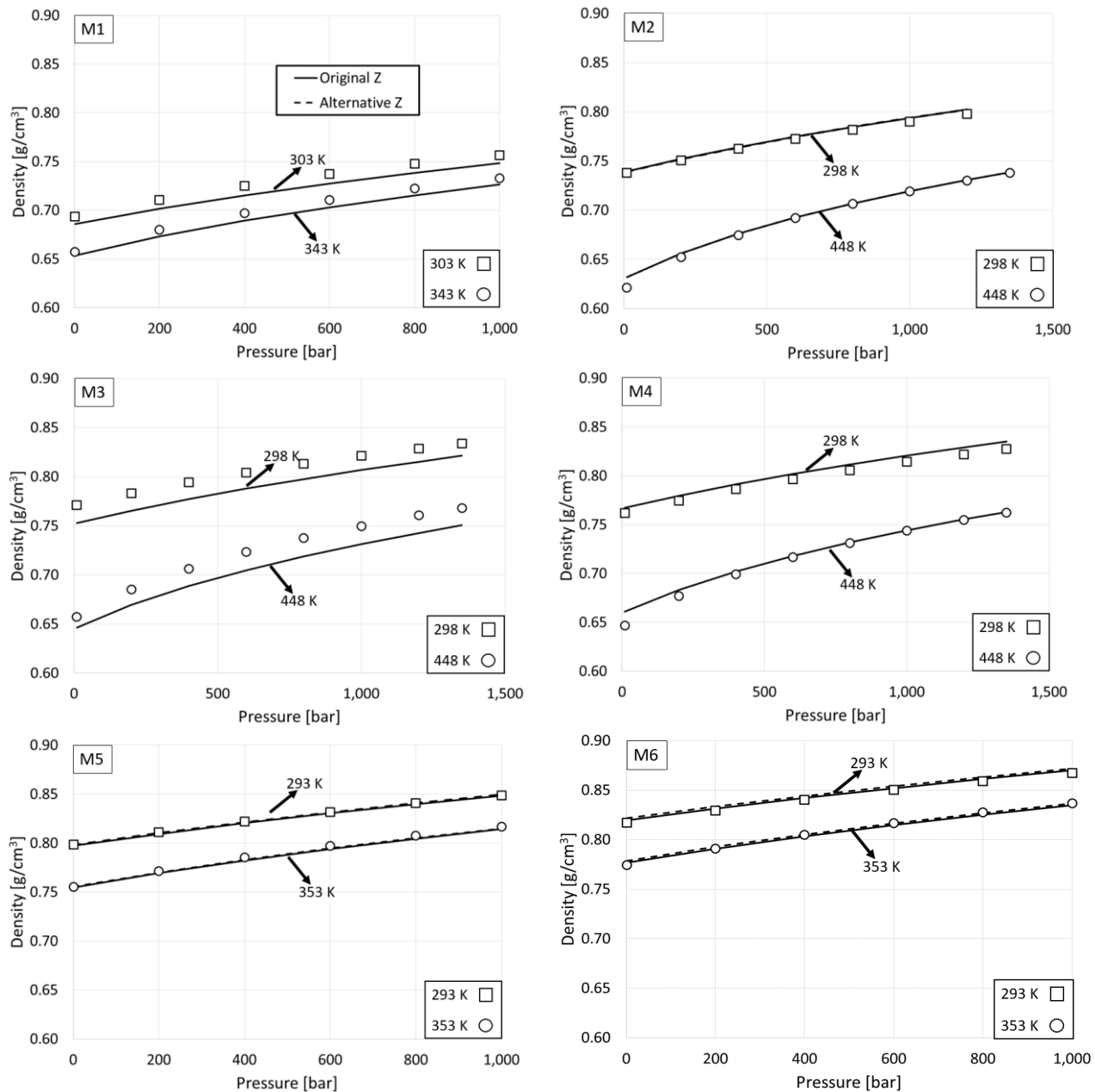


Figure 3. Density predictions (lines) compared to experimental data [63-65] (symbols) for hydrocarbon mixtures.

Table 4 shows statistical measures for density predictions of the binary mixture (M1) with MAPDs ranging from 0.2 to 2.5%, with an average MAPD of 1.2% for all considered mixture compositions. The MAPDs of the density predictions appear to increase monotonically with increasing mole fraction of MCH. This behavior could

potentially be due to the relatively low MW of n-heptane and MCH, both of which lie at the extreme lower bound of fitted PC-SAFT correlations. Large concentrations of these compounds are not typically found in diesel and jet fuels.

Mole fraction					
$x_{n\text{-heptane}}$	$x_{\text{MCH}}$	MAPD	Bias	SD	Max D
1.000	0.000	0.2	0.2	0.2	0.9
0.875	0.125	0.4	-0.4	0.2	0.6
0.750	0.250	1.1	-1.1	0.2	1.3
0.625	0.375	1.8	-1.8	0.2	2.1
0.500	0.500	2.5	-2.5	0.1	2.7
Average		1.2	-1.1	0.9	2.7

Table 4. The MAPD (%), bias (%), SD (%), and Max D (%) for density predictions of the M1 hydrocarbon mixture with different compositions of methyl-cyclohexane (MCH) and n-heptane.

Table 5 summarizes the density predictions using the original and alternative Z equations for the calculation of the PC-SAFT parameters for the ternary, quaternary, and quinary mixtures studied by Ijaz [64] and Boned et al. [65] (the M2-M6 mixtures). The density predictions show that the original and alternative equations used to calculate Z provide similarly accurate predictions for these well-defined simple mixtures.

Mixture	Z	MAPD	Bias	SD	Max D
M2	Original	0.3	0.3	0.3	1.8
M3	Original	2.2	-2.2	0.2	2.4
M4	Original	0.6	0.6	0.4	2.4
M5	Original	0.2	-0.2	0.1	0.5
	Alternative	0.1	-0.1	0.1	0.3
M6	Original	0.2	0.0	0.1	1.0
	Alternative	0.3	-0.3	0.2	0.6

Table 5. The MAPD (%), bias (%), SD (%), and Max D (%) for density predictions of M2-M6 hydrocarbon mixtures. When the number averaged MW of the mixture is less than the MW of phenanthrene, Eq. 7 reduces to Eq. 2, and the original and alternative Z parameters are the same.

Direct experimental measurement of the isothermal compressibility ( $\kappa_T$ ) and volumetric thermal expansion coefficient ( $\alpha_p$ ) is challenging, which is reflected in limited data available in the literature. Therefore, density data are fit to the Tait equation, Eq. 13, and the isothermal compressibility (Eq. 14) and volumetric thermal expansion coefficient (Eq. 15) are calculated from derivatives of the Tait fits to density.

$$\frac{\rho - \rho_0(T)}{\rho} = A \log_{10} \left( \frac{P + B(T)}{P_0 + B(T)} \right) \quad (13)$$

$$\kappa_T = \frac{1}{\rho} \left( \frac{d\rho}{dP} \right)_T \quad (14)$$

$$\alpha_p = -\frac{1}{\rho} \left( \frac{d\rho}{dT} \right)_P \quad (15)$$

In Eq. 13,  $\rho_0$  is the density at the reference pressure of 0.1 MPa,  $B$  is a temperature dependent parameter, and  $A$  is a constant. Values for  $\rho_0$  and  $B$  fit to each isotherm were subsequently fit to second order polynomials as a function of temperature, Eq. 16 and 17.

$$\rho_0(T) = \sum_{i=0}^2 e_i T^i \quad (16)$$

$$B(T) = \sum_{i=0}^2 b_i T^i \quad (17)$$

MAPDs less than 0.10%, biases less than -0.02%, SDs less than 0.10%, and Max Ds less than 0.47% are obtained between data and predictions using the Tait equation for the mixtures considered here. Values for  $A$  and the coefficients in Eq. 16 and 17 for all of the mixtures are found in the SI. For brevity, only the composition containing 0.750 mole fraction n-heptane and 0.250 mole fraction MCH are reported in the following figures. Figure 4 presents the predicted mixture  $\kappa_T$  compared to Tait calculations from experimental density data. The effects of temperature and pressure are well predicted quantitatively.

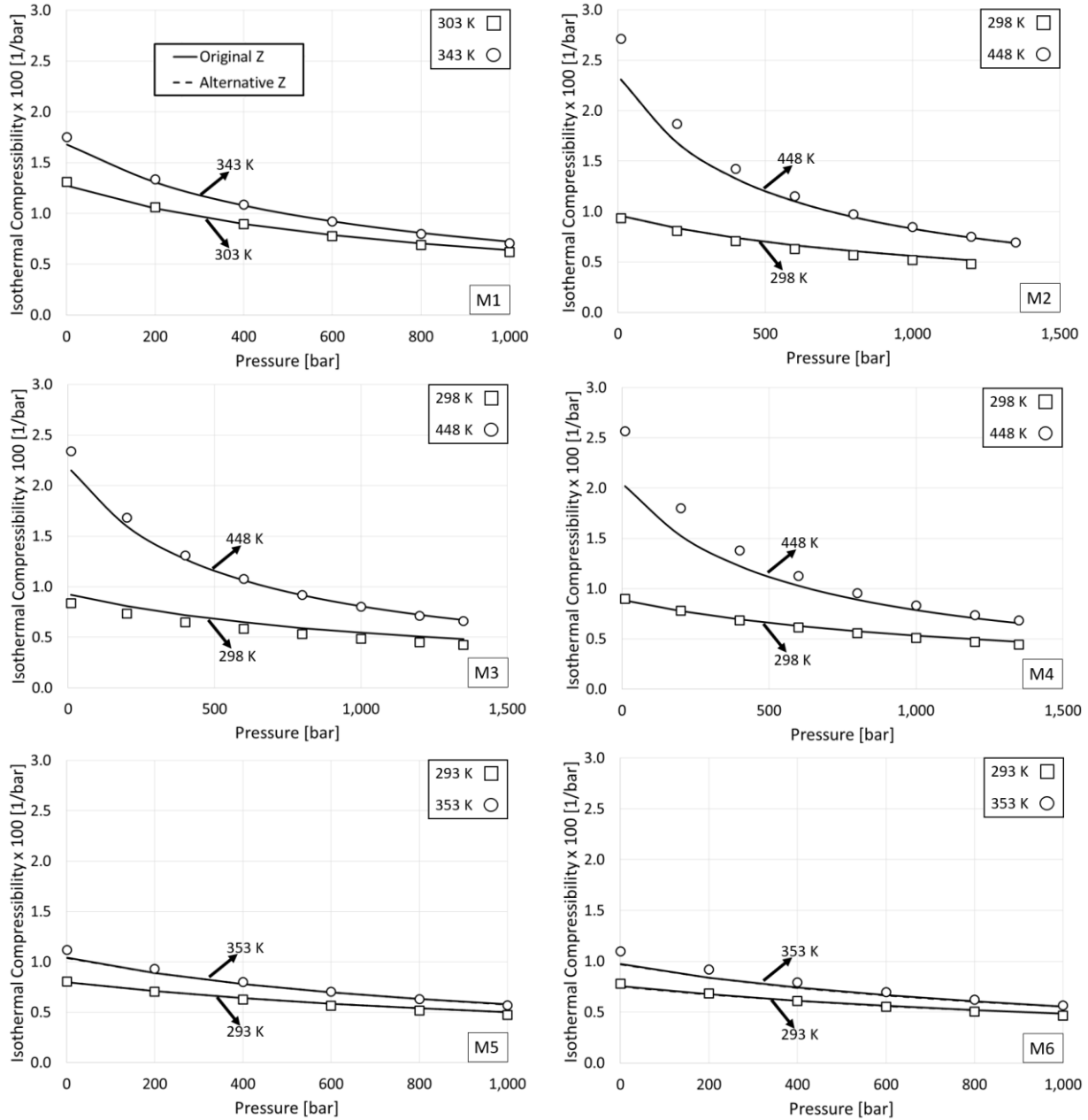


Figure 4. Isothermal compressibility predictions (lines) compared to experimental data [63-65] (symbols) for hydrocarbon mixtures.

Figure 5 shows predictions for  $\alpha_p$  compared to Tait calculations from experimental density data. The predictions capture the qualitative trends with respect to pressure, with the coefficients monotonically decreasing with pressure for all mixtures. The predictions capture the qualitative trends with respect to temperature for the M1-M4 mixtures.

Predictions for the M5 and M6 mixtures exhibit an inverse dependence on temperature for all pressures compared to the Tait calculations. A crossover in temperature is observed between 200 and 500 bar for the M1-M4 mixtures for predictions and the Tait calculations. A crossover in temperature is observed for the Tait calculations at pressures less than 200 bar and pressures between 200 and 400 bar for the M5 and M6 mixtures, respectively, but is not observed in the predictions. For pressures below the crossover point,  $\alpha_p$  increases with temperature, and for pressures above the crossover point,  $\alpha_p$  decreases with temperature. Previous studies observed a crossover in temperature at pressures less than 600 bar for benzene, tetrachloromethane, hexane, nonane, dodecane, tridecane, pentadecane, mixtures of trialkylimidazolium-based ionic liquids, biodiesel from rapeseed oil, and standard petroleum diesel oil [66-69]. The crossover has been attributed to anharmonicity of intermolecular vibrations [66-68].

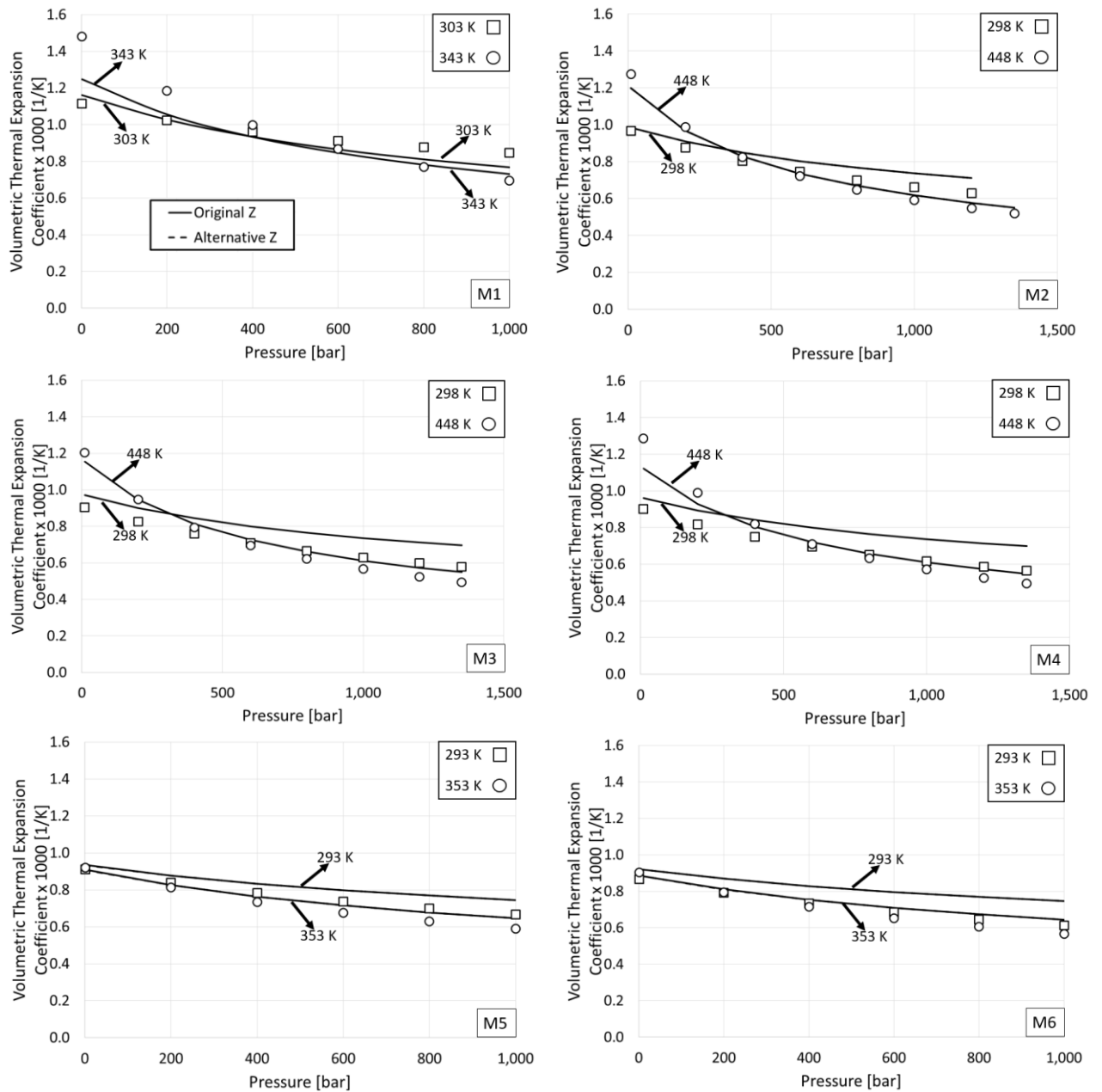


Figure 5. Volumetric thermal expansion coefficient predictions (lines) compared to experimental data [63-65] (symbols) for hydrocarbon mixtures.

Tables 6 and 7 summarize statistical measures for the  $\kappa_T$  and  $\alpha_p$  predictions using the original and alternative Z equations for the calculation of the PC-SAFT parameters for the M1-M6 mixtures. The alternative equation used to calculate Z does not significantly impact predictions of the derivative properties.

Mixture	Z	MAPD	Bias	SD	Max D
M1	Original	1.9	-0.2	1.4	5.6
M2	Original	3.8	-0.7	3.3	14.9
M3	Original	5.6	4.5	3.6	13.2
M4	Original	5.2	-3.5	4.7	20.1
M5	Original	2.5	0.2	1.8	6.7
	Alternative	2.5	0.0	1.8	7.1
M6	Original	3.6	-2.6	2.9	11.5
	Alternative	3.7	-2.7	3.0	12.0

Table 6. The MAPD (%), bias (%), SD (%), and Max D (%) for isothermal compressibility predictions of hydrocarbon mixtures.

Mixture	Z	MAPD	Bias	SD	Max D
M1	Original	7.2	-5.8	3.7	21.9
M2	Original	4.0	1.3	2.8	13.1
M3	Original	6.3	5.2	4.7	20.5
M4	Original	6.8	3.1	5.5	23.8
M5	Original	5.3	5.1	3.2	11.8
	Alternative	5.3	5.1	3.2	11.8
M6	Original	9.9	9.8	5.7	22.0
	Alternative	9.9	9.8	5.7	22.0

Table 7. The MAPD (%), bias (%), SD (%), and Max D (%) for volumetric thermal expansion coefficient predictions of hydrocarbon mixtures.

### 3 Diesel and Jet Fuels

Commercially available distillate fuels (*e.g.*, diesel, gasoline, kerosene, jet fuels) are composed of hundreds of hydrocarbons. Composition depends on the source of the crude oil, distillation conditions, target fuel quality specifications [70, 71], and additional processing and blending with additives. Table 8 lists the limited number of experimental studies reporting the density of diesel and jet fuels up to HTHP conditions. Outcalt and

colleagues [72, 73] measured the density of jet fuels JP-8 3773 (referred to as JP-8) and Jet A 4658 (referred to as Jet A) at high temperatures between 270 and 470 K and pressures up to 400 bar. Safarov et al. [74] reported density measurements of the Hallen DK B0 diesel fuel from 2015 (referred to as B02015) and 2016 (referred to as B02016) over a wide range of temperatures between 263 and 468 K and pressures up to 2,000 bar. Aquing et al. [35] measured the density of the Middle East SR and Highly Naphthenic diesel fuels at temperatures between 323 and 423 K and pressures up to 3,500 bar.

Reference	Year	Fuel	T <sub>range</sub> /K	P <sub>range</sub> /bar	Density uncertainty (%)	No. of samples with measured composition
Peters et al. <sup>[75]</sup>	1990	Diesel	299-450	To 1,000	-	0
Payri et al. <sup>[76]</sup>	2011	Diesel	298-343	To 1,800	0.60	0
Aqing et al. <sup>[35]</sup>	2012	Diesel	323-423	To 3,500	0.05	2
Bazile et al. <sup>[77]</sup>	2012	Diesel	283-423	To 2,000	0.01	0
Schaschke et al. <sup>[78]</sup>	2013	Diesel	298-373	To 5,000	0.20	0
Desantes et al. <sup>[79]</sup>	2015	Diesel	303-353	To 2,000	0.01	0
Ivaniš et al. <sup>[80]</sup>	2016	Diesel	293-413	To 600	0.01	0
Safarov et al. <sup>[74]</sup>	2018	Diesel	263-468	To 2,000	0.04	2 <sup>[81]</sup>
Outcalt et al. <sup>[72]</sup>	2009	Jet	278-343	To 320	0.01	1 <sup>a</sup>
Outcalt et al. <sup>[73]</sup>	2010	Jet	278-343	To 400	0.01	1 <sup>b</sup>
Abdulagatov and Azizov <sup>[82]</sup>	2010	Jet	301-745	To 600	0.10	0

<sup>a</sup>Number averaged MW and  $\text{HN}/\text{CN}$  from ref. [83].

<sup>b</sup>Number averaged MW and  $\text{HN}/\text{CN}$  from ref. [84].

Table 8. Summary of available density data for diesel and jet fuels measured up to high temperatures and pressures.

Aqing et al. [35] used gas chromatography to characterize the composition of the chemical families in the two diesel fuels shown in Table 9. One of the fuels is a conventional diesel fuel distilled from Middle Eastern crude oil (Middle East Straight

Run (SR)) and the other is a fuel treated after distillation to hydrogenate aromatic compounds (Highly Naphthenic). Saturated compounds (*i.e.*, normal alkanes, branched alkanes, cyclohexanes, and decalins) comprise 70 mol% of the Middle East SR diesel fuel and 65 mol% of the Highly Naphthenic diesel fuel. There is a significant difference in concentrations of naphthenes (*i.e.*, cyclohexanes and decalins) and alkanes between the two diesel fuels. The Middle East SR diesel fuel contains 20 mol% naphthenes and about 50 mol% normal and branched alkanes compared to 46 mol% naphthenes and 20 mol% normal and branched alkanes in the Highly Naphthenic diesel fuel. Figure 6 shows the MW distribution of the 140 different compounds identified in these diesel fuels. The MWs of compounds in the Middle East SR diesel fuel range from 100 to 370 g/mol with the majority of compounds having MWs between 150 to 300 g/mol. The MW distribution of the Highly Naphthenic diesel fuel is wider from 100 to 480 g/mol. However, the majority of compounds have lower MWs between 100 to 260 g/mol, as compared to the Middle East SR diesel fuel. Although not shown here, compositional variability is also observed between the different jet fuels reported in the literature [35, 85, 86]. The composition of the Hallen DK B0 diesel fuel was not reported [74], but the average MW and HN/CN ratio were obtained from private communication [81].

Chemical class	Mole percent (%)		Carbon number range	
	Middle East SR	Highly Naphthenic	Middle East SR	Highly Naphthenic
Normal alkanes	23	6	7-27	7-29
Branched alkanes	26	13	7-27	7-29
Cyclohexanes	16	26	8-26	8-28
Decalins	4	20	10-25	10-26
Benzenes	10	10	8-24	8-20
Naphthalenes	7	3	10-21	10-15
Phenanthrenes	3	1	14-20	14-35
Tetralins + Indanes	7	16	9-23	9-22
Other unsaturates	4	5	12-21	13-35

Table 9. Molar composition (%) and carbon number ranges of chemical families found in Middle East SR and Highly Naphthenic diesel fuels obtained from gas chromatography. Data from ref. [35].

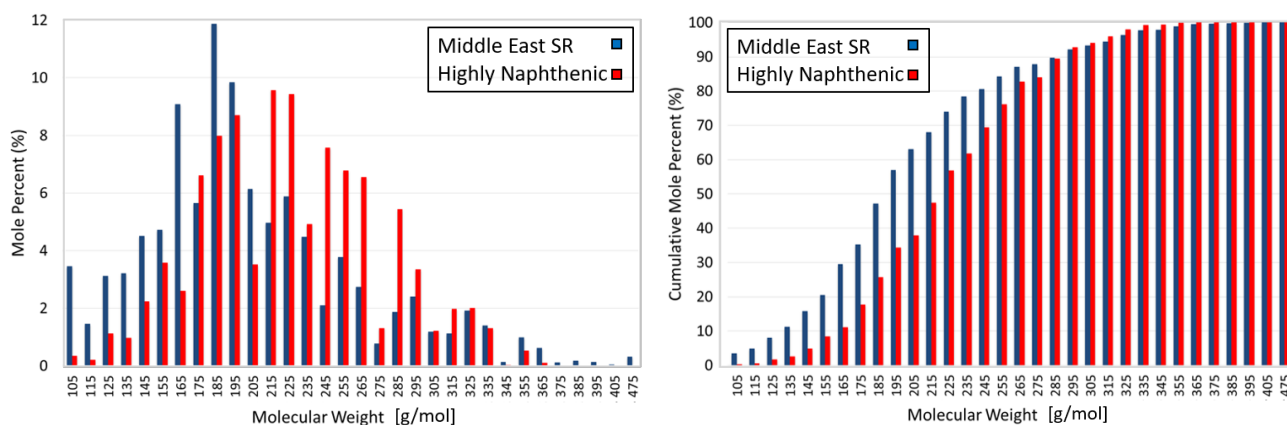


Figure 6. Molecular weight distribution (left) and cumulative mole percent (right) of the compounds in Middle East SR and Highly Naphthenic diesel fuels from gas chromatography. Data from ref. [35].

Table 10 presents the mixture properties for the four diesel fuels and two jet fuels in this study, the  $Z$  parameter, and the PC-SAFT parameters of the pseudo-components for both combinations of approaches.

Sample	MW	HN/CN	PC-SAFT parameters				
			Z		$m$	$\sigma$ (Å)	$\varepsilon/k$ (K)
Middle East SR	225.1 <sup>a</sup>	1.85 <sup>a</sup>	Original	0.1731	9.7335	3.4085	258.44
			Alternative	0.2217	9.6111	3.4053	263.11
Highly Naphthenic	203.6 <sup>a</sup>	1.74 <sup>a</sup>	Original	0.2537	8.7269	3.3959	263.24
			Alternative	0.2923	8.6422	3.3928	266.77
B0 2015	215.0	1.92	Original	0.1294	9.4471	3.4087	253.17
			Alternative	0.1579	9.3796	3.4067	255.85
B0 2016	215.0	1.92	Original	0.1294	9.4471	3.4087	253.17
			Alternative	0.1579	9.3796	3.4067	255.85
JP-8 3773	160.0 <sup>b</sup>	1.95 <sup>b</sup>	Original	0.1444	7.2656	3.3872	246.33
			Alternative	0.1444	7.2656	3.3872	246.33
Jet A4658	157.5 <sup>c</sup>	1.96 <sup>c</sup>	Original	0.1399	7.1747	3.3864	245.47
			Alternative	0.1399	7.1747	3.3864	245.47

<sup>a</sup>From the gas chromatography results from ref. [35].

<sup>b</sup>From ref. [84].

<sup>c</sup>From ref. [83].

Table 10. Mixture properties and PC-SAFT parameters for the pseudo-components of diesel and jet fuels predicted in this study. When the number averaged MW of the mixture is less than the MW of phenanthrene, Eq. 7 reduces to Eq. 2, and the original and alternative Z parameters are the same.

Figure 7 shows the predictions and experimental density data for the four diesel fuels and the two jet fuels at the lowest and highest temperatures and a range of pressures. The predictions are in quantitative agreement with experimental data across all temperatures and pressures for all six fuels. Table 11 summarizes the statistical measures for the four diesel and two jet fuels, for all temperatures and pressures, using the original and alternative equations for calculating Z needed to calculate the PC-SAFT parameters. The use of the alternative equation for Z improves the accuracy of the density predictions for all of the diesel fuels. However, improvement is not observed for the jet fuel density

predictions since the MW of these fuels is less than the MW of phenanthrene, and the alternative Z equation (Eq. 7) reduces to the original equation (Eq. 2).

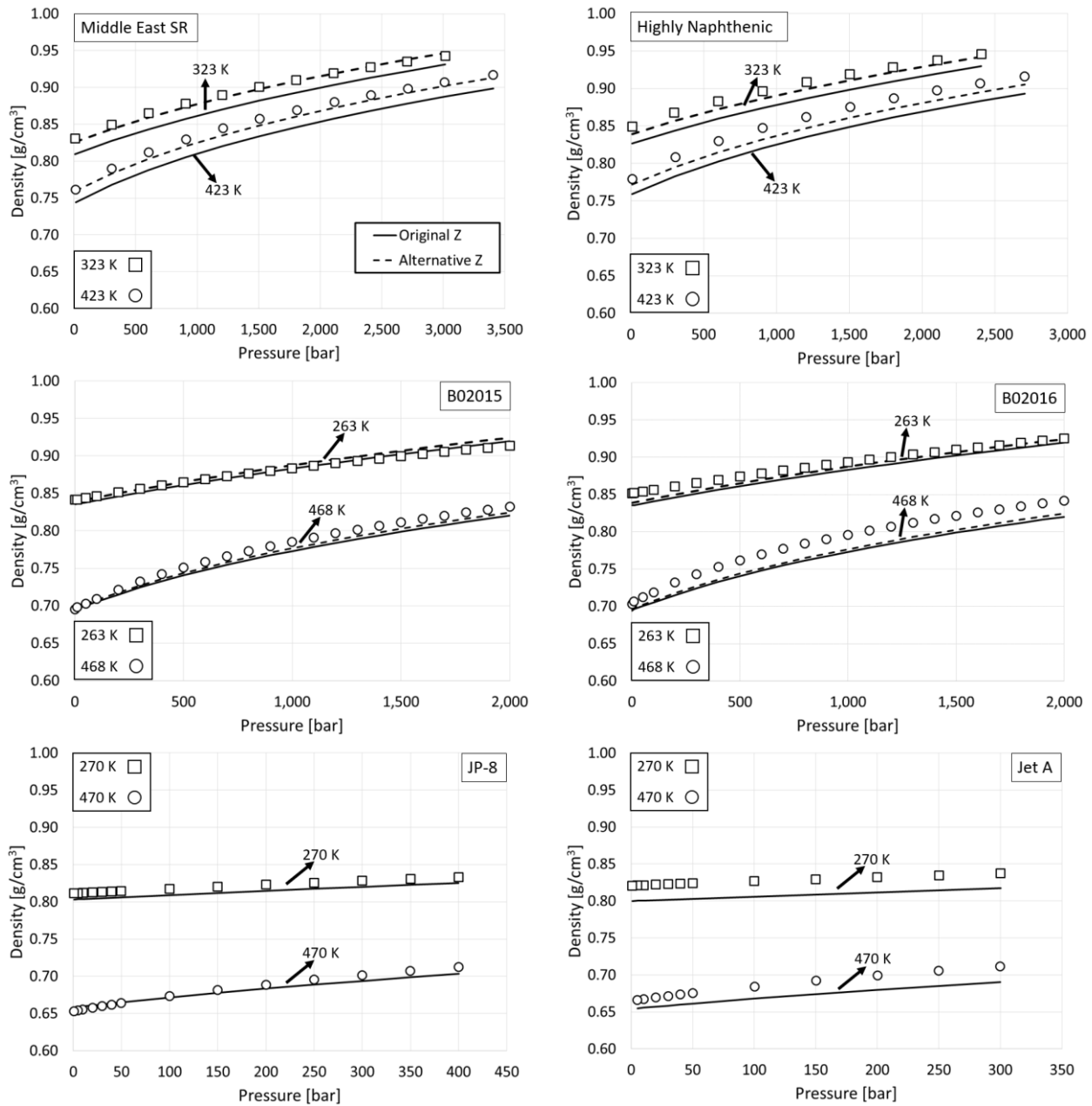


Figure 7. Density predictions (lines) compared to experimental data [35, 72-74] (symbols) for diesel and jet fuels.

Sample	Z	MAPD	Bias	SD	Max D
Middle East SR	Original	2.3	-2.3	0.4	3.0
	Alternative	0.6	-0.6	0.3	1.1
Highly Naphthenic	Original	2.6	-2.6	0.4	3.2
	Alternative	1.2	-1.2	0.4	1.8
B02015	Original	1.0	-1.0	0.4	1.6
	Alternative	0.4	0.0	0.3	1.7
B02016	Original	2.2	-2.2	0.5	2.9
	Alternative	1.2	-1.2	0.5	1.9
JP-8	Original	1.1	-1.1	0.3	1.4
	Alternative	1.1	-1.1	0.3	1.4
Jet A	Original	2.6	-2.6	0.3	3.0
	Alternative	2.6	-2.6	0.3	3.0

Table 11. The MAPD (%), bias (%), SD (%), and Max D (%) for density predictions of diesel and jet fuels.

The same approach used for the hydrocarbon mixtures is applied to predict the derivative properties of the fuels. The  $A$  constant and the coefficients in Eq. 16 and 17 for the Tait equation fit to diesel and jet fuel density data are included in the SI. Figure 8 shows the predicted isothermal compressibilities ( $\kappa_T$ ) for the fuels compared to Tait calculations from the experimental density data. Predictions are in quantitative agreement with experimental data. However, the model overpredicts at the lowest temperatures and underpredicts at the highest temperatures. Although the predictions in Figure 8 for fuels JP-8 and Jet A appear to exhibit a greater deviation compared to predictions for the diesel fuels, note that x-axes are scaled differently in the figures. The MAPDs reported for the  $\kappa_T$  predictions in Table 12 show similar values for the diesel and jet fuels. The alternative equation for calculating  $Z$  does not significantly improve the  $\kappa_T$  predictions for the fuels studied in this work.

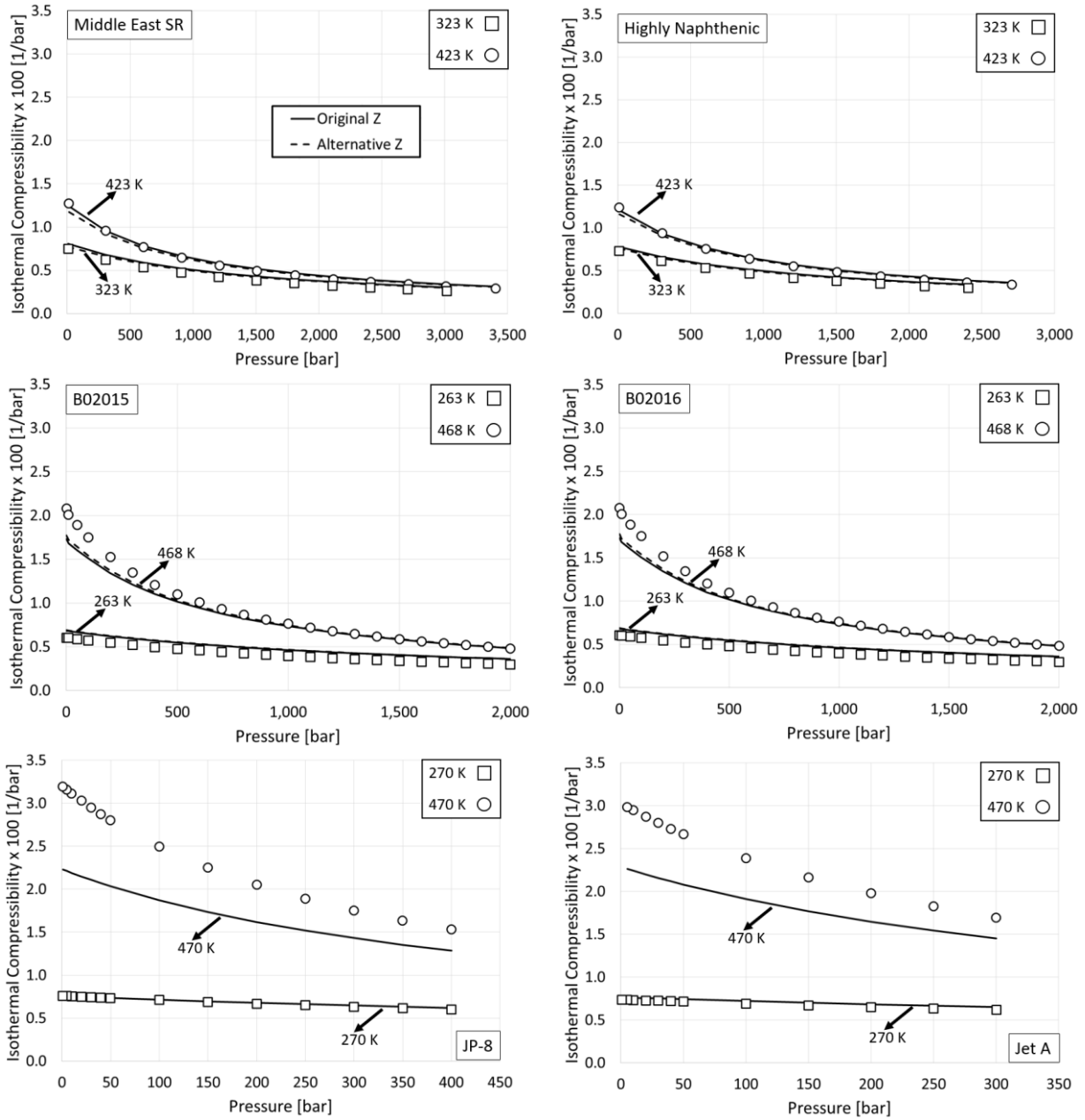


Figure 8. Isothermal compressibility predictions (lines) compared to experimental data [35, 72-74] (symbols) for diesel and jet fuels.

Sample	Z	MAPD	Bias	SD	Max D
Middle East SR	Original	8.0	7.8	4.3	16.3
	Alternative	6.4	5.3	3.9	14.8
Highly Naphthenic	Original	7.1	6.9	3.8	14.4
	Alternative	5.7	4.8	3.5	13.0
B02015	Original	14.8	14.8	3.8	21.3
	Alternative	13.1	13.1	4.2	20.2
B02016	Original	14.5	14.5	3.9	21.0
	Alternative	12.8	12.8	4.3	20.0
JP-8	Original	13.8	-13.6	8.7	30.3
	Alternative	13.8	-13.6	8.7	30.3
Jet A	Original	11.1	-10.1	7.3	24.2
	Alternative	11.1	-10.1	7.3	24.2

Table 12. The MAPD (%), bias (%), SD (%), and Max D (%) for isothermal compressibility predictions of diesel and jet fuels.

Figure 9 shows predicted volumetric thermal expansion coefficients ( $\alpha_p$ ) compared to Tait calculations from the experimental density data. The predictions for all of the fuels qualitatively capture the observed monotonic decrease in  $\alpha_p$  with respect to pressure. All of the predictions for all fuels show better agreement at higher temperatures compared to lower temperatures.

The Tait calculations for the Highly Naphthenic diesel fuel exhibit a temperature crossover between 300 and 600 bar. However, this crossover is not observed with the Middle East SR diesel fuel. In contrast, a predicted temperature crossover is observed for both of these diesel fuels, but at a pressure less than 50 bar. Predicted  $\alpha_p$  values exhibit more sensitivity to temperature than experimental values obtained with Tait calculations. Similar trends are observed with predicted  $\alpha_p$  values for the B02015 and B02016 diesel fuels, although now the predicted temperature crossover occurs at pressures less than 10

bar. In contrast the predicted  $\alpha_p$  for Jet fuels JP-8 and Jet A show a temperature crossover temperature at approximately 200 bar. However, Tait calculations for  $\alpha_p$ , for these four fuels, do not exhibit a temperature crossover.

Table 13 summarizes the statistical measures for predictions of the volumetric thermal expansion coefficient for the four diesel fuels and two jet fuels using the original and alternative approaches for calculating  $Z$  for the calculation of the PC-SAFT parameters. For the volumetric thermal expansion coefficient calculations, the alternative approach for calculating  $Z$  does not significantly improve the predictions for the fuels studied in this work.

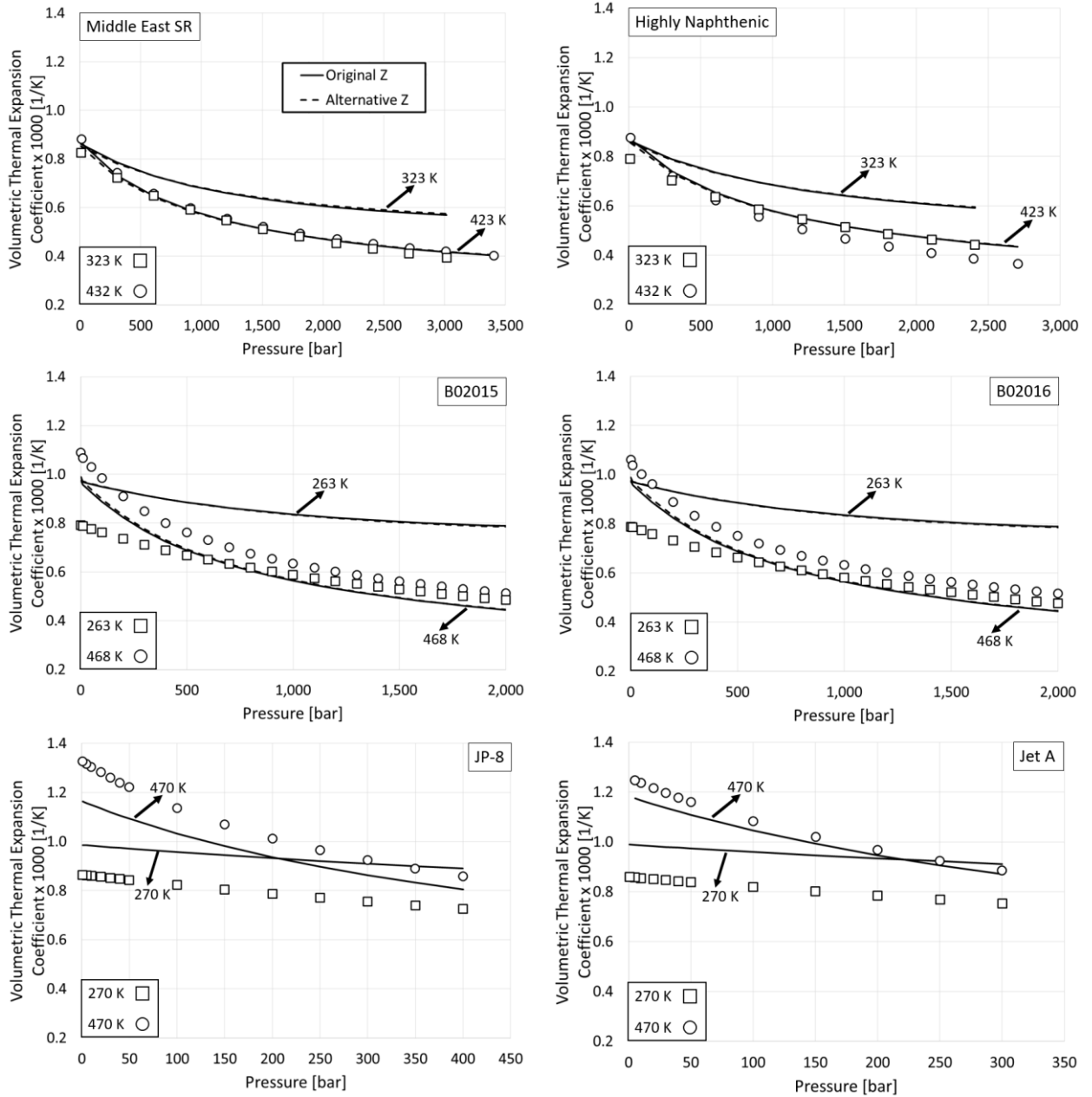


Figure 9. Volumetric thermal expansion coefficient predictions (lines) compared to experimental data [35, 72-74] (symbols) for diesel and jet fuels.

Sample	Z	MAPD	Bias	SD	Max D
Middle East SR	Original	13.3	12.3	13.2	44.9
	Alternative	13.7	12.4	13.6	46.2
Highly Naphthenic	Original	14.6	14.6	8.6	33.8
	Alternative	14.6	14.5	9.0	34.5
B02015	Original	14.2	11.7	15.5	62.6
	Alternative	14.3	11.5	15.7	63.5
B02016	Original	17.4	14.0	14.6	65.5
	Alternative	17.5	13.8	14.7	66.4
JP-8	Original	7.9	-2.3	4.8	22.6
	Alternative	7.9	-2.3	4.8	22.6
Jet A	Original	5.8	0.3	4.6	21.1
	Alternative	5.8	0.3	4.6	21.1

Table 13. The MAPD (%), bias (%), SD (%), and Max D (%) for volumetric thermal expansion coefficient predictions of diesel and jet fuels.

A discussion is found in the SI on the potential sources of error in the derivative property predictions. Lafitte et al. [87] suggest that the inaccuracy in derivative property calculations is a result of the intermolecular potential used in the PC-SAFT EoS. Predictions can be improved if a Mie potential is used instead of the square-well potential used in PC-SAFT. The Mie potential is used in more recent SAFT variants (*i.e.*, SAFT for variable range interactions with Mie potentials (SAFT-VR Mie[88]) and SAFT- $\gamma$ -Mie [89]). However, these SAFT variants are not currently as widely used in industry as is PC-SAFT. Predictions could also be improved by simultaneously regressing the PC-SAFT parameters (or the GC parameters) to both density and derivative properties, similar to the approach of de Villiers et al. [29]. Much broader data sets are needed such as saturated liquid density, isochoric heat capacity, vapor pressure, enthalpy of vaporization, and speed of sound as used by de Villiers et al. [29].

## 4 Conclusion

A purely predictive, single, pseudo-component technique using the Perturbed-Chain Statistical Associating Fluid Theory (PC-SAFT) equation of state was developed to predict the density, isothermal compressibility, and volumetric thermal expansion coefficient of complex hydrocarbon mixtures, such as diesel and jet fuels. This approach negates the need for fitting binary interaction parameters to experimental mixture data. The method in this study is predictive up to high temperatures and pressures, without the need to fit parameters to experimental data. The approach described here only requires the input of two calculated or experimentally measured mixture properties: the number averaged molecular weight and the hydrogen to carbon ratio. We speculate that further improvements in the accuracy of this pseudo-component technique, especially for derivative property estimations, can be realized if a different variant of the SAFT equation of state is used, such as SAFT-VR Mie [88] or SAFT- $\gamma$ -Mie [89]. However, these SAFT variants are not as widely applied in industrial practice, and to be used with the pseudo-component technique, it would be necessary to develop a set of correlations specific to these equations of state. The purely predictive, single, pseudo-component technique described here provides a straightforward, yet powerful, tool to aid the development of improved fuel injection equipment design and control. This tool will also aid the development and optimization of fuel and fluid formulations for improved performance at extreme operating conditions.

## Acknowledgements

This project has received funding from the European Union Horizon 2020 Research and Innovation program, Grant Agreement No 675528. The authors wish to thank Joseph

Roos (Afton), Joseph Remias (Afton), Mark Devlin (Afton), and Rajendar Mallepally (VCU) for their helpful, technical discussions.

## List of symbols

### *English symbols*

$\bar{a}$	reduced Helmholtz free energy	$k$	Boltzmann constant
$m$	segment number	$P$	pressure
$T$	temperature	CN	carbon number
HN	hydrogen number	$y$	evaluated property
$N$	number of data points	$X$	mole fraction
$B$	temperature dependent parameter in Eq. 13	$A$	a constant in Eq. 13
$Z$	normalized degree of unsaturation	HN/CN	hydrogen to carbon ratio
$e$	coefficients in Eq. 16	$b$	coefficients in Eq. 17

### *Greek symbols*

$\varepsilon/k$	depth of potential well	$\sigma$	segment diameter
$\rho$	density	$\alpha_p$	volumetric thermal expansion coefficient
$\kappa_T$	isothermal compressibility	$\gamma$	exponent in the Mie potential

### *Superscripts*

$res$	residual	$hc$	hard-chain
$disp$	dispersion		

## References

1. Tat ME, Van Gerpen JH, Soyly S, Canakci M, Monyem A, Wormley S. The speed of sound and isentropic bulk modulus of biodiesel at 21 C from atmospheric pressure to 35 MPa. *Journal of the American Oil Chemists' Society*. 2000; 77: p. 285–289.
2. Hoekman SK, Robbins C. Review of the effects of biodiesel on NOx emissions. *Fuel Processing Technology*. 2012; 96: p. 237–249.
3. Lapuerta M, Armas O, Rodriguez-Fernandez J. Effect of biodiesel fuels on diesel engine emissions. *Progress in Energy and Combustion Science*. 2008; 34: p. 198–223.

4. Wei M, Li S, Xiao H, Guo G. Combustion performance and pollutant emissions analysis using diesel/gasoline/iso-butanol blends in a diesel engine. *Energy Conversion and Management*. 2017; 149: p. 381-391.
5. Tavlarides LL, Antiescu G, inventors; Supercritical diesel fuel composition, combustion process and fuel system. US patent 7,488,357. 2009.
6. Vogel T, Götz G, Wensing M. Transition of fuel components into supercritical state under diesel process conditions. In *Proc 25th ILASS Europe*; 2013; Chania.
7. Lemaire R, Faccineto A, Therssen E, Ziskind M, Focsa C, Desgroux P. Experimental comparison of soot formation in turbulent flames of diesel and surrogate diesel fuels. In *Proceedings of the Combustion Institute*; 2009.
8. Luning Prak DJ, Alexandre SM, Cowart JS, Trulove PC. Density, viscosity, speed of sound, bulk modulus, surface tension, and flash point of binary mixtures of n-dodecane with 2, 2, 4, 6, 6-pentamethylheptane or 2, 2, 4, 4, 6, 8, 8-heptamethylnonane. *Journal of Chemical & Engineering Data*. 2014; 59: p. 1334–1346.
9. Nayyar A, Sharma D, Soni SL, Mathur A. Characterization of n-butanol diesel blends on a small size variable compression ratio diesel engine: modeling and experimental investigation.. *Energy Conversion and Management*. 2017; 150: p. 242-258.
10. Nabi MN, Zare A, Hossain FM, Bodisco TA, Ristovski ZD, Brown RJ. A parametric study on engine performance and emissions with neat diesel and diesel-butanol blends in the 13-Mode European Stationary Cycle. *Energy conversion and management*. 2017; 148: p. 251-259.
11. Mueller CJ, Cannella WJ, Bruno TJ, Bunting B, Dettman HD, Franz JA, et al. Methodology for formulating diesel surrogate fuels with accurate compositional, ignition-quality, and volatility characteristics. *Energy & Fuels*. 2012; 26: p. 3284–3303.
12. Luning Prak DJ, Morris RE, Cowart JS, Hamilton LJ, Trulove PC. Density, viscosity, speed of sound, bulk modulus, surface tension, and flash point of Direct Sugar to Hydrocarbon Diesel (DSH-76) and binary mixtures of n-hexadecane and 2, 2, 4, 6, 6-pentamethylheptane. *Journal of Chemical & Engineering Data*. 2013; 58: p. 3536–3544.
13. Srivastava SP, Hancok J. *Fuels and Fuel-Additives*: John Wiley & Sons; 2014.
14. Lemmon EW, Huber ML. Thermodynamic properties of n-dodecane. *Energy & Fuels*. 2004; 18: p. 960–967.
15. Gieleciak R. GCxGC studies of palette compounds used in the next generation of diesel fuel surrogate blends. ; 2016.
16. Theodorakakos A, Mitroglou N, Atkin C, Gavaises M. Friction-induced heating in nozzle hole micro-channels under extreme fuel pressurisation. *FUEL*. 2014; 123: p. 143-150.
17. Strotos G, Koukouvinis P, Theodorakakos A, Gavaises M, Bergeles G. Transient heating effects in high pressure Diesel injector nozzles. *International Journal of Heat and Fluid Flow*. 2015; 51: p. 257–267.
18. Strotos G, Malgarinos I, Nikolopoulos N, Gavaises M. Predicting the evaporation rate of stationary droplets with the VOF methodology for a wide range of ambient temperature conditions. *International Journal of Thermal Sciences*. .
19. Murali Girija M, Koukouvinis P, Gavaises M. A simultaneous numerical simulation of cavitation and atomization using a fully compressible three-phase model. *Physical Review Fluids*. 2018.
20. Kolev N. Diesel Fuel Properties. In *Multiphase Flow Dynamics 3: Turbulence, Gas Absorption and Release*.: Springer; 2002.
21. Lemmon EW, Huber ML, McLinden MO. NIST Reference fluid thermodynamic and transport properties database (REFPROP). 2013..
22. Sudiro M, Bertuccio A. roduction of synthetic gasoline and diesel fuel by alternative processes using natural gas and coal: Process simulation and optimization. *Energy*. 2009; 34: p. 2206–2214.
23. Ely JF, Huber ML. NIST thermophysical properties of hydrocarbon mixtures database (SUPERTRAPP). 2007..

24. Lin R, Tavlarides LL. Thermophysical properties needed for the development of the supercritical diesel combustion technology: Evaluation of diesel fuel surrogate models. *The Journal of Supercritical Fluids*. 2012; 71: p. 136–146.
25. Stamataki S, Tassios D. Performance of cubic EOS at high pressures. *Revue de l'Institut Français du Pétrole*. 1998; 53: p. 367–377.
26. Pedersen K, Milter J, Sørensen H. Cubic equations of state applied to HT/HP and highly aromatic fluids. In *SPE Annual Technical Conference and Exhibition*; 2002.
27. Gross J, Sadowski G. Perturbed-chain SAFT: An equation of state based on a perturbation theory for chain molecules. *Industrial & Engineering Chemistry Research*. 2001; 40: p. 1244–1260.
28. Kontogeorgis GM, Folas GK. Appendix A. In *Thermodynamic models for industrial applications: from classical and advanced mixing rules to association theories.*: John Wiley & Sons; 2009.
29. Liang X, Yan W, Thomsen K, Kontogeorgis GM. On petroleum fluid characterization with the PC-SAFT equation of state. *Fluid Phase Equilibria*. 2014; 375: p. 254–268.
30. Tihic A, Kontogeorgis GM, von Solms N, Michelsen ML, Constantinou L. A predictive group-contribution simplified PC-SAFT equation of state: application to polymer systems. *Industrial & Engineering Chemistry Research*. 2007; 47: p. 5092–5101.
31. De Villiers A, Schwarz C, Burger A, Kontogeorgis G. Evaluation of the PC-SAFT, SAFT and CPA equations of state in predicting derivative properties of selected non-polar and hydrogen-bonding compounds. *Fluid Phase Equilibria*. 2013; 338: p. 1–15.
32. Leekumjorn S, Krejbjerg K. Phase behavior of reservoir fluids: Comparisons of PC-SAFT and cubic EOS simulations. *Fluid Phase Equilibria*. 2013; 359: p. 17–23.
33. Peng DY, Robinson DB. A new two-constant equation of state. *Industrial & Engineering Chemistry Fundamentals*. 1976; 15: p. 59–64.
34. Soave G. Equilibrium constants from a modified Redlich-Kwong equation of state. *Chemical Engineering Science*. 1972; 27: p. 1197–1203.
35. Yan W, Varzandeh F, Stenby EH. PVT modeling of reservoir fluids using PC-SAFT EoS and Soave-BWR EoS. *Fluid Phase Equilibria*. 2015; 386: p. 96–124.
36. Burgess WA, Tapriyal D, Morreale BD, Soong Y, Baled HO, Enick RM, et al. Volume-translated cubic EoS and PC-SAFT density models and a free volume-based viscosity model for hydrocarbons at extreme temperature and pressure conditions. *Fluid Phase Equilibria*. 2013; 359: p. 38–44.
37. Schou Pedersen K, Hasdbjerg C. PC-SAFT equation of state applied to petroleum reservoir fluids. In *SPE Annual Technical Conference and Exhibition*; 2007.
38. Gord MF, Roozbahani M, Rahbari HR, Hosseini SJH. Modeling thermodynamic properties of natural gas mixtures using perturbed-chain statistical associating fluid theory. *Russian Journal of Applied Chemistry*. 2013; 86: p. 867–878.
39. Panuganti SR, Vargas FM, Gonzalez DL, Kurup AS, Chapman WG. PC-SAFT characterization of crude oils and modeling of asphaltene phase behavior. *Fuel*. 2012; 93: p. 658–669.
40. Zúñiga-Hinojosa MA, Justo-García DN, Aquino-Olivos MA, Román-Ramírez LA, García-Sánchez F. Modeling of asphaltene precipitation from n-alkane diluted heavy oils and bitumens using the PC-SAFT equation of state. *Fluid Phase Equilibria*. 2014; 376: p. 210–224.
41. Mueller CJ, Cannella WJ, Bays JT, Bruno TJ, DeFabio K, Dettman HD, et al. Diesel surrogate fuels for engine testing and chemical-kinetic modeling: Compositions and properties. *Energy & Fuels*. 2016; 30: p. 1445–1461.
42. Puduppakkam K, Naik C, Meeks E, Krenn C, Kroiss R, Gelbmann J, et al. Predictive Combustion and Emissions Simulations for a High Performance Diesel Engine Using a Detailed Fuel Combustion Model. ; 2014.
43. Prediction for Tetradecahydrophenanthrene from Chemspider. [Online]. [cited 2017 May 30. Available from: <http://www.chemspider.com/Chemical-Structure.20647.html>.
44. Wertheim M. Fluids with highly directional attractive forces. I. Statistical thermodynamics. *Journal of Statistical Physics*. 1984; 35: p. 19–34.

45. Wertheim M. Fluids with highly directional attractive forces. II. Thermodynamic perturbation theory and integral equations. *Journal of Statistical Physics*. 1984; 35: p. 35–47.
46. Wertheim M. Fluids with highly directional attractive forces. III. Multiple attraction sites. *Journal of Statistical Physics*. 1986; 42: p. 459–476.
47. Wertheim M. Fluids with highly directional attractive forces. IV. Equilibrium polymerization. *Journal of Statistical Physics*. 1986; 42: p. 477–492.
48. Lorentz H. Über die anwendung des satzes vom virial in der kinetischen theorie der gase. *Annalen der Physik*. 1881; 248: p. 127–136.
49. Tapriyal D, Enick R, McHugh M, Gamwo I, Morreale B. High Temperature, high pressure equation of state density correlations and viscosity correlations. ; 2012.
50. Justo-García DN, García-Sánchez F, Romero-Martínez A, Díaz-Herrera E, Juaristi E. Isothermal Multiphase Flash Calculations with the PC-SAFT Equation of State. In *AIP Conference Proceedings*; 2008.
51. Baker LE, Pierce AC, Luks KD. Gibbs energy analysis of phase equilibria. *Society of Petroleum Engineers Journal*. 1982; 22: p. 731–42.
52. Michelsen ML. The isothermal flash problem. Part I. Stability. *Fluid phase equilibria*. 1982; 9: p. 1–9.
53. Fletcher R. Unconstrained Optimization Wiley. In *Practical Methods of Optimization*. Vol. 1.: Wiley Interscience; 1980.
54. Baled HO, Gamwo IK, Enick RM, McHugh MA. Viscosity models for pure hydrocarbons at extreme conditions: A review and comparative study. *Fuel*. 2018; 218: p. 89–111.
55. Lohrenz J, Bray BG, Clark CR. Calculating viscosities of reservoir fluids from their compositions. *Journal of Petroleum Technology*. 1964; 16: p. 1171–1176.
56. Quiñones-Cisneros SE, Zéberg-Mikkelsen CK, Fernández J, García J. General friction theory viscosity model for the PC-SAFT equation of state. *AIChE Journal*. 2006; 52: p. 1600–1610.
57. Llovell F, Marcos R, Vega L. Free-volume theory coupled with soft-SAFT for viscosity calculations: comparison with molecular simulation and experimental data. *The Journal of Physical Chemistry B*. 2013; 117: p. 8159–8171.
58. Yarranton HW, Satyro MA. Expanded fluid-based viscosity correlation for hydro- carbons. *Industrial & Engineering Chemistry Research*. 2009; 48: p. 3640–3648.
59. Chung TH, Ajlan M, Lee LL, Starling KE. Generalized multiparameter correlation for nonpolar and polar fluid transport properties. *Industrial & Engineering Chemistry Research*. 1988; 27: p. 671–679.
60. Pedersen KS, Fredenslund A. An improved corresponding states model for the prediction of oil and gas viscosities and thermal conductivities. *Chemical Engineering Science*. 1984; 39: p. 1011–1016.
61. Lotgering-Lin O, Gross J. Group contribution method for viscosities based on entropy scaling using the perturbed-chain polar statistical associating fluid theory. *Industrial & Engineering Chemistry Research*. 2015; 54: p. 7942–7952.
62. Rosenfeld Y. Relation between the transport coefficients and the internal entropy of simple systems. *Physical Review A*. 1977; 15: p. 2545.
63. Chapman S, Cowling TG. The mathematical theory of non-uniform gases: an account of the kinetic theory of viscosity, thermal conduction and diffusion in gases. ; 1970.
64. Sauer E, Stavrou M, Gross J. Comparison between a homo-and a heterosegmented group contribution approach based on the perturbed-chain polar statistical associating fluid theory equation of state. *Industrial & Engineering Chemistry Research*. 2014; 53: p. 14854–14864.
65. Novak LT. Predicting natural gas viscosity with a mixture viscosity model for the entire fluid region. *Industrial & Engineering Chemistry Research*. 2013; 52: p. 16014–16018.
66. Grunberg L, Nissan AH. Mixture law for viscosity. *Nature*. 1949; 164: p. 799–800.
67. Schaschke C, Fletcher I, Glen N. Density and viscosity measurement of diesel fuels at combined high pressure and elevated temperature. *Processes*. 2013; 1: p. 30–48.
68. Poling BE, Prausnitz JM, John Paul O, Reid RC. *The properties of gases and liquids* New York: McGraw-Hill; 2001.

69. Wu X, Li C, Jia W. An improved viscosity model based on Peng-Robinson equation of state for light hydrocarbon liquids and gases. *Fluid Phase Equilibria*. 2014; 380: p. 147-151.
70. Rowane AJ. High-Temperature, High-Pressure viscosities and densities of toluene; MS Thesis. ; 2016.
71. American Society for Testing and Materials. Standard specification for diesel fuel oils D975. ; 2011.
72. Bedoya ID, Arrieta AAA, Cadavid F. Effects of mixing system and pilot fuel quality on diesel-biogas dual fuel engine performance. *Bioresource Technology*. 2009; 100: p. 6624-6629.